

# Isotopically diverse rhyolites coeval with the Columbia River Flood Basalts: evidence for mantle plume interaction with the continental crust

Dylan P. Colón,<sup>1</sup> Ilya N. Bindeman,<sup>1</sup> Richard A. Stern<sup>2</sup> and Chris M. Fisher<sup>3</sup>

<sup>1</sup>Department of Geological Sciences, 1272 University of Oregon, Eugene, OR 97402, USA; <sup>2</sup>Department of Earth and Atmospheric Sciences, University of Alberta, 1-26 Earth Sciences Building, Edmonton, AB, Canada; <sup>3</sup>School of the Environment, Washington State University, PO Box 642812, Pullman, WA, USA

## ABSTRACT

The Columbia River Flood Basalts (CRB) of the northwestern USA are coeval with eruptions of several thousand km<sup>3</sup> of rhyolite. A broad survey of major phenocryst oxygen isotopes and of O and Hf isotopes in zircons from these rhyolites reveals significant diversity in inferred  $\delta^{18}\text{O}_{\text{melt}}$  values, ranging from +1.9 to +10.5‰ (SMOW), and in zircon Hf isotope compositions, which range from  $\varepsilon_{\text{Hf}} = -39$  to +9. This newly identified isotopic diversity shows that the syn-CRB rhyolites were derived from high-percentage melting of the crust. Low- $\delta^{18}\text{O}$  rhyolites, which fingerprint the melting of

hydrothermally altered crust, are concentrated at the edge of the North American craton. This suggests that the conditions of crustal heating, faulting, and hydrothermal alteration required for the production of these rhyolites were concentrated there by the contrasts in crustal thickness and rheology associated with the boundary between the North American craton and younger accreted terranes.

Terra Nova, 00: 1–7, 2015

## Introduction

Continental bimodal large igneous provinces are widely considered to be the product of interaction between mantle plumes and the crust (Bryan and Ferrari, 2013 and references therein). The youngest of these, the Columbia River Basalts (CRB), was produced by the Yellowstone mantle plume (e.g. Duncan, 1982; Glen and Ponce, 2002; Camp and Ross, 2004; Schmandt *et al.*, 2012). The first eruptions of the CRB occurred in thin accreted oceanic crust at Steens Mountain at 16.7–16.5 Ma (Camp *et al.*, 2003, 2015; Reidel *et al.*, 2013), and were quickly followed by the earliest syn-CRB silicic volcanism: the 16.55 Ma Tuff of Oregon Canyon at the McDermitt centre (Fig. 1, Coble and Mahood, 2012). As with the basalts, silicic volcanism was widespread (Fig. 1) until 14.5 Ma, when it became focused on the Snake River Plain hotspot track. Syn-CRB rhyolitic volcanism occurred in compositionally diverse accreted oceanic terranes west of the  $^{87}\text{Sr}/^{86}\text{Sr} = 0.706$  isopleth (Fig. 1, Dorsey and LaMa-

skin, 2008; Leeman *et al.*, 1992) and in older cratonic crust to the east. In this study, we use oxygen and radiogenic isotopes to determine the origin of these rhyolites and to further understand how the Yellowstone mantle plume modified the composition and structure of this complex crust during the flood basalt event.

## Samples and analytical methods

We collected and analysed ~50 samples of CRB and syn-CRB rhyolites (details in the Supporting Information). Major phenocrysts were picked from whole rock samples that were crushed and treated with cold hydrofluoric acid (HF) for 80–100 min to remove glass and its alteration products. Zircons were also hand-picked from a subset of syn-CRB rhyolites after dissolving most other material in HF over a period of 2 days. Zircon is particularly useful as it is highly resistant to weathering that may alter the chemical and isotopic composition of the whole rock and major phenocrysts. The  $\delta^{18}\text{O}$  values of major phenocrysts in basalts and rhyolites were measured via laser fluorination at the University of Oregon (Bindeman, 2008) with precision better than  $\pm 0.1\text{‰}$ . Zircon  $\delta^{18}\text{O}$  was measured in situ using the CAMECA 1280R ion microprobe at the

University of Alberta ( $\pm 0.1\text{--}0.2\text{‰}$ ), and a subset of these were analysed in overlapping spots for Hf isotope compositions by laser ablation ICP-MS at Washington State University ( $\pm 1\text{--}2 \varepsilon$  units). XRF and ICP-MS analyses of major and trace elements were also performed for selected units. Detailed methods appear in the Supporting Information.

## Results

We report the first mineral  $\delta^{18}\text{O}$  analyses for olivine and plagioclase from the CRB, with values ranging from slightly below to normal mantle-like values (average  $\delta^{18}\text{O}_{\text{olivine}} = +4.9$  to  $+5.1\text{‰}$  and average  $\delta^{18}\text{O}_{\text{plagioclase}} = 5.5\text{--}6.0\text{‰}$  SMOW) in the Picture Gorge basalts to somewhat higher (average  $\delta^{18}\text{O}_{\text{olivine}} = 5.7\text{‰}$  and  $\delta^{18}\text{O}_{\text{plagioclase}} = +5.7$  to  $+6.6\text{‰}$ ) values for Steens, Imnaha, and Grande Ronde basalts (Fig. 2a). Computed equilibrium melt  $\delta^{18}\text{O}$  values (bulk including phenocrysts, see Supporting Information) for these phenocrysts broadly overlap with whole rock measurements by Carlson (1984). The ash flow tuffs of the High Rock ( $\delta^{18}\text{O}$  from Mallis *et al.*, 2014; all other values this study) and McDermitt caldera complexes, the Dinner Creek Tuff, lava domes west of Steens Mountain, and

Correspondence: Dylan P. Colón, Department of Geological Sciences, 1272 University of Oregon, Eugene, OR 97402, USA. Tel.: +1 608 630 4700; e-mail: dcolon@uoregon.edu

COLOR

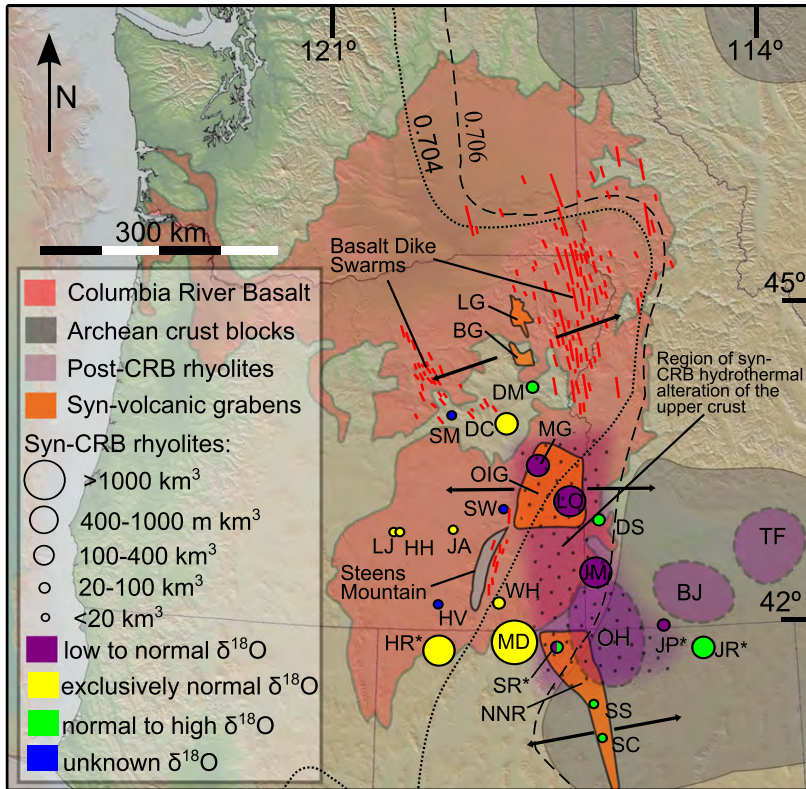


**Fig. 1** Map of the volcanism that occurred over the Yellowstone plume head from 17 to 14 Ma. Syn-CRB rhyolite eruptive centres are solid circles: DeLamar-Silver City (DS), Dinner Creek Tuff eruptive centre (DC), Dooley Mountain (DM), Hawks Valley-Lone Mountain (HV), High Rock (HR), Horsehead Mountain (HH), Jackass Butte (JA), J-P Desert (JP), Jarbidge Rhyolite (JR), Juniper Mountain (JM), Lake Owyhee (LO), Little Juniper Mountain (LJ), Malheur Gorge (MG), McDermitt (MD), Santa Rosa-Calico (SR), Sheep Creek Range (SC), Snowstorm Mountains (SS), Strawberry Mountains (SM), Swamp Creek (SW) and Whitehorse (WH) (estimates of erupted volume from Coble and Mahood, 2012). Younger Snake River Plain caldera complexes at Owyhee-Humboldt (OH), Bruneau-Jarbidge (BJ) and Twin Falls (TF) are shown in light purple. All  $\delta^{18}\text{O}$  data are from this study, with the exception of values for the High Rock (Mallis *et al.*, 2014) and Santa Rosa-Calico centres (Amrhein *et al.*, 2013) and the J-P Desert and Jarbidge rhyolites (see Colón *et al.*, 2015; for a discussion of these rhyolites' inclusion with the syn-CRB group), which are emphasised by asterisks in the figure. Syn-volcanic grabens that make up the north-south trending zone of extension that parallels the edge of the craton include the Baker Graben (BG), the La Grande graben (LG), the Northern Nevada Rift, and the Oregon-Idaho graben (OIG). The latter sits on the edge of the suture zone of transitional crust between oceanic and continental lithosphere defined by the  $^{87}\text{Sr}/^{86}\text{Sr} = 0.706$  and  $0.704$  isopleths, emphasised by the locations of Archean crustal blocks just to the east, explaining the isotopically diverse magmatism there (Fig. 2). See the Supporting Information for detailed sample locations.

many large-volume lava flows of the Lake Owyhee Volcanic Field have normal to slightly high  $\delta^{18}\text{O}$  values ( $\delta^{18}\text{O}_{\text{melt}} = +6.0$  to  $+8.0\text{‰}$ ). In contrast, we observe low- $\delta^{18}\text{O}_{\text{melt}}$  values in syn-CRB rhyolites that erupted in and near the Oregon-Idaho graben

along the terrane-craton boundary (Fig. 1), including the major caldera-forming ignimbrites of the Lake Owyhee volcanic field, the Tuff of Spring Creek ( $\delta^{18}\text{O}_{\text{melt}} = +4.0\text{‰}$ ) and the Tuff of Leslie Gulch ( $\delta^{18}\text{O}_{\text{melt}} = +4.8\text{‰}$ ), and the Littlefield

and Cottonwood Mountain Rhyolites of the Malheur Gorge region ( $\delta^{18}\text{O}_{\text{melt}} = +2.6$ – $2.7$  and  $+1.9$ – $2.8\text{‰}$ , respectively), all of which have volumes of 100–400  $\text{km}^3$  (Fig. 1, Coble and Mahood, 2012). High  $\delta^{18}\text{O}$  values ( $>+8.0\text{‰}$ ) are observed in syn-CRB rhyolites from the Silver City, Northern Nevada Rift and Dooley Mountain centres (Fig. 1), with the latter having  $\delta^{18}\text{O}_{\text{melt}}$  values as high as  $+10.5\text{‰}$  (Fig. 2), some of the highest  $\delta^{18}\text{O}$  values measured in volcanic rock (e.g. Bindeman, 2008). The range in  $\delta^{18}\text{O}$  values in the syn-CRB rhyolites therefore greatly exceeds the range measured in the Columbia River Basalts themselves (Fig. 2) as well as the range in the basalts and rhyolites of the Snake River Plain (Bindeman and Simakin, 2014), reflecting similar observations of  $\delta^{18}\text{O}$  diversity in the syn-CRB rhyolites of central Oregon by Jenkins *et al.* (2013).

Zircons in syn-CRB rhyolites display an even greater range of  $\delta^{18}\text{O}$  values than the associated major phenocrysts, with values as low as  $-0.6\text{‰}$  in the J-P Desert (Colón *et al.*, 2015) and as high as  $+10.8\text{‰}$  at Dooley Mountain (Fig. 2). Furthermore, zircons in syn-CRB rhyolites exhibit a variability of  $>1\text{‰}$  in  $\delta^{18}\text{O}$ , well in excess of analytical uncertainties for single spots (Fig. 2), implying disequilibrium  $\Delta^{18}\text{O}_{\text{melt-zircon}}$  values for many grains (such as the  $+1.65\text{‰}$  zircon in the Tuff of Spring Creek, with  $\Delta^{18}\text{O}_{\text{melt-zircon}} = +2.3\text{‰}$ , or the  $+10.8\text{‰}$  zircon from a rhyolitic dike in Dooley Mountain, with  $\Delta^{18}\text{O}_{\text{melt-zircon}} = -0.3\text{‰}$ , both compared to an equilibrium  $\Delta^{18}\text{O}_{\text{melt-zircon}}$  of  $\sim+1.7\text{‰}$  for typical  $900\text{ °C}$  rhyolite, Bindeman, 2008). One particularly extreme example of zircon diversity comes from the J-P Desert locality (Fig. 1), described in Colón *et al.* (2015). There, individual eruptive units contain zircons with a range of up to  $6\text{‰}$   $\delta^{18}\text{O}$  and  $30\ \epsilon_{\text{HF}}$  units, with severe  $\Delta^{18}\text{O}_{\text{melt-zircon}}$  disequilibrium. Finally, zircons from rhyolites erupted through or near to the cratonic crust east of the  $^{87}\text{Sr}/^{86}\text{Sr} = 0.706$  line (including the J-P Desert) have lower  $\epsilon_{\text{HF}}$  values than those from rhyolites erupted through accreted terranes to the west (Fig. 3, e.g. Nash *et al.*, 2006 for whole rocks).

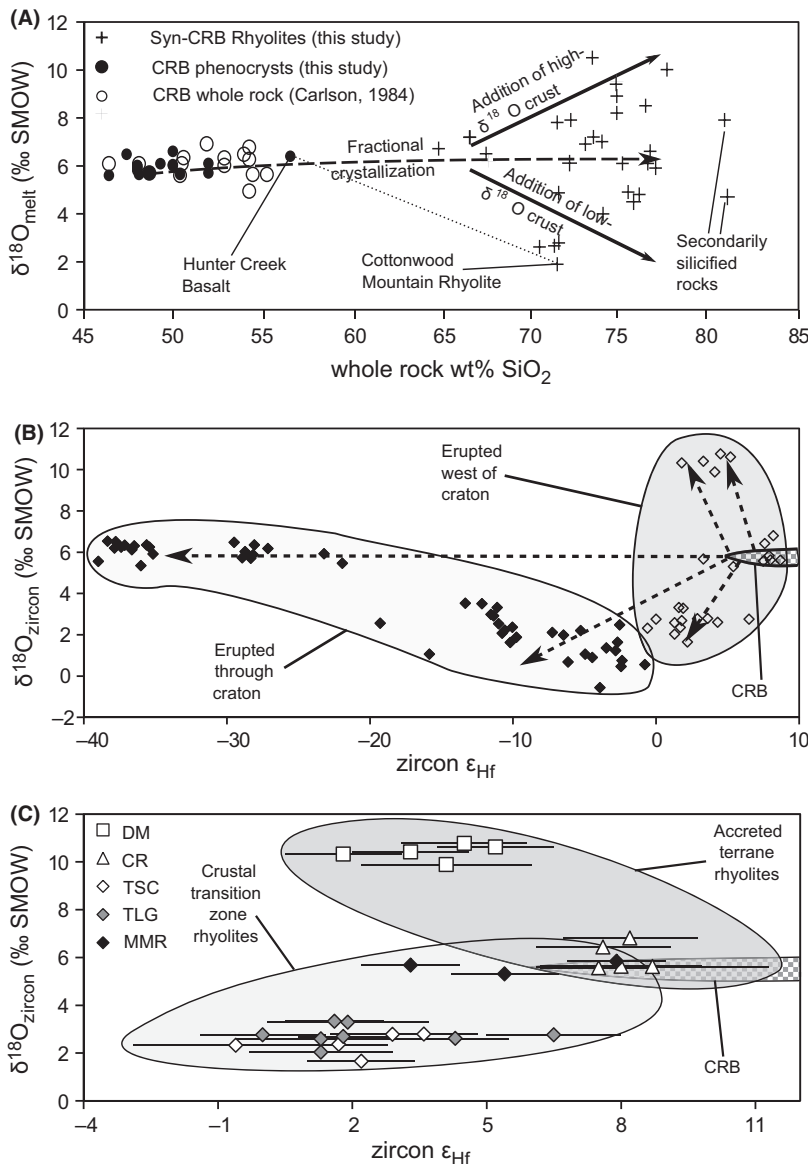


**Fig. 2** Isotopic and chemical trends in syn-CRB rhyolites. (a) Silica content vs.  $\delta^{18}\text{O}_{\text{melt}}$  for CRB and syn-CRB rhyolites. The curve showing the expected evolution of  $\delta^{18}\text{O}_{\text{melt}}$  during fractional crystallisation is from Bindeman (2008). The spread of  $\delta^{18}\text{O}_{\text{melt}}$  values away from this curve is the result of extensive melting of diverse- $\delta^{18}\text{O}$  crust into the evolving syn-CRB rhyolite magmas. Two coeval units, the low- $\delta^{18}\text{O}$  Cottonwood Mountain Rhyolite and the relatively high- $\delta^{18}\text{O}$  Hunter Creek Basalt (both of the Malheur Gorge region), are highlighted to emphasise their contrasting compositions. (b) Zircon  $\delta^{18}\text{O}$  and  $\epsilon_{\text{Hf}}$  values for a subset of the syn-CRB rhyolites. Data for zircons in rhyolites that erupted through the craton are from Colón *et al.* (2015). These zircons show much greater diversity in  $\epsilon_{\text{Hf}}$  values due to the influence of very old and unradiogenic Archaean crust (Fig. 1). (c) Detail of zircon compositions of syn-CRB rhyolites that erupted through accreted terranes west of the craton boundary, including zircons from Dooley Mountain (DM), the Dinner Creek Tuff (DC), the Tuffs of Spring Creek (TSC) and Leslie Gulch (TLG) and the Mahogany Mountain Rhyolite (MMR) (the latter three from the Lake Owyhee volcanic field, LO). The three Lake Owyhee units erupted through the transition zone between the craton and the younger accreted terranes to the west, reflected by lower  $\delta^{18}\text{O}$  values (Fig. 3). By contrast, the units that erupted farther from the edge of the craton (DM and DC) have normal to high  $\delta^{18}\text{O}$  values and generally higher  $\epsilon_{\text{Hf}}$  values, reflecting the melting of younger accreted crust.

## Discussion

### High and low- $\delta^{18}\text{O}$ rhyolites: evidence for large-scale plume-driven crustal remelting

The scatter in  $\delta^{18}\text{O}_{\text{melt}}$  values away from the normal mantle value of 5.7‰ in much of the CRB is consistent with models that implicate the contribution of remelts of lithospheric material in the formation of the CRB (e.g. Hooper and Hawkesworth, 1993; Camp and Hanan, 2008; Wolff *et al.*, 2008; Wolff and Ramos, 2013). Similarly, the much larger variation in major phenocryst  $\delta^{18}\text{O}$  values in the syn-CRB rhyolites suggests that they are derived from remelting of pre-existing continental crust. Both the syn-CRB rhyolites and the Snake River Plain rhyolites require a minimum crustal melt contribution of 15–40% by volume (Leeman, 1982; Nash *et al.*, 2006; McCurry and Rodgers, 2009) and many are likely up to 80% crustal melt (Bindeman and Simakin, 2014; Colón *et al.*, 2015). The syn-CRB rhyolites extend into higher  $\delta^{18}\text{O}$  values than those of the Snake River Plain (e.g. Bindeman and Simakin, 2014), and many high- $\delta^{18}\text{O}$  rhyolites, such as those erupted at Dooley Mountain, are likely derived from melting regionally abundant high- $\delta^{18}\text{O}$  sedimentary or metasedimentary protoliths. By contrast, at Silver City, Idaho, high- $\delta^{18}\text{O}$  rhyolites ( $\delta^{18}\text{O}_{\text{qtz}} = +8.6$  to  $+10.2$ ‰) are likely derived from melting of local high- $\delta^{18}\text{O}$  Cretaceous granitoids ( $\delta^{18}\text{O}_{\text{qtz}} = +10.4$ ‰), implying up to 80% crustal melt in their formation (Supporting Information). Low- $\delta^{18}\text{O}$  rhyolites, on the other hand, are derived from the remelting of precursor rocks that have been hydrothermally altered by hot meteoric water at large water/rock ratios (e.g. Taylor, 1974). Like their high- $\delta^{18}\text{O}$  counterparts, low- $\delta^{18}\text{O}$  rhyolites (+1.8 to +5.5‰) require 10–50% contributions of crustal remelts for their formation, based on the lower bound of  $\delta^{18}\text{O}$  values observed for typical hydrothermally altered rocks ( $\sim 0$ ‰) that could melt to form them (e.g. Bindeman and Simakin, 2014, and references therein).

Hf isotopes in zircon from rhyolites that erupted through cratonic

COLOR

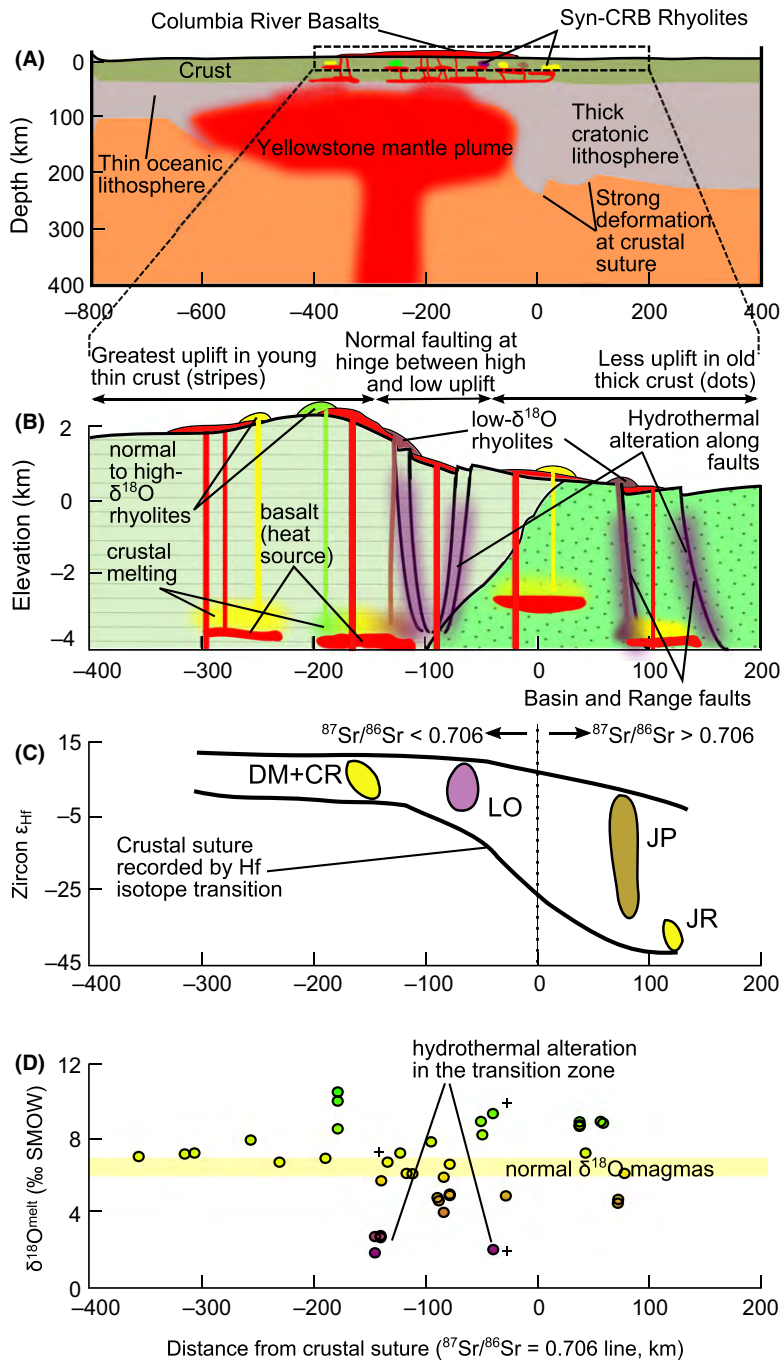


**Fig. 3** Plume influence on the continental crust through tectonism and melt production at the suture between the thick craton and thin, young accreted terranes. (a) The plume asymmetrically flattens against the steep edge of the thick continental lithosphere, causing extensive deformation and crustal heating to be concentrated along this boundary. (b) Surface uplift is concentrated where the lithosphere is thin and is minimal in the thick lithosphere, creating a flexure zone at the suture where the two crustal types and uplift regimes meet. Meteoric water intrudes into the crust via normal faults in this flexure zone, which can also serve as conduits for erupting rhyolitic magmas. Rising magmas melt crust that is hydrothermally altered by the interaction of meteoric water and country rock driven by heat from deeper intrusions, producing low- $\delta^{18}O$  rhyolites (parts a–b) are modified from the models of Burov *et al.*, 2007). (c) The transition between old crust and young accreted crust is recorded by Hf isotopes in syn-CRB rhyolites in the area, consistent with similar step-function behaviour in radiogenic isotopes in rhyolites observed by Nash *et al.* (2006). (d) Finally, the concentration of heating and deformation at the transition zone near the crustal boundary leads to the proliferation of hydrothermal alteration of the crust and low- $\delta^{18}O$  rhyolite production in that area. By contrast, syn-CRB rhyolites that erupted to the west of the zone of normal faulting and hydrothermal alteration have normal to high  $\delta^{18}O$  values. The plus symbols are from Amrhein *et al.* (2013) and Mallis *et al.* (2014), and parts (c–d) also contain data from Colón *et al.* (2015).

crust (Figs 1 and 2) are frequently highly unradiogenic, indicating the involvement of melts of Precambrian crust (Colón *et al.*, 2015). Hf in zircon from rhyolites that erupted through young accreted terranes is less diagnostic of crustal melting, but the abundance of low- $\delta^{18}\text{O}$  values in high- $\epsilon_{\text{Hf}}$  crust (this study, Colón *et al.*, 2015; Seligman *et al.*, 2014) suggests that hydrothermal alteration affects young porous rocks more than older and presumably impermeable metamorphic rocks, similar to what is observed at the Skaergaard intrusion (Norton and Taylor, 1979). The so-called ‘Nd–O paradox’ observed in the Snake River Plain (McCurry and Rodgers, 2009; Ellis *et al.*, 2013), in which normal  $\delta^{18}\text{O}$  rocks have high  $\epsilon_{\text{Hf}}$  and  $\epsilon_{\text{Nd}}$  values, and vice versa, can be explained by this simple relationship. Finally, the diversity in zircon isotopic compositions in single units reflects the eruption of mixtures of crustal melt batches before the zircons can reset to equilibrium values (e.g. Bindeman and Simakin, 2014; Colón *et al.*, 2015).

### Plume-driven crustal hydrothermal alteration

The production of low- $\delta^{18}\text{O}$  rhyolites is generally constrained to shallow depths, as meteoric water will lose its low- $\delta^{18}\text{O}$  composition due to equilibration with the country rocks before reaching depths of 5–10 km (Drew *et al.*, 2013; Bindeman and Simakin, 2014; Seligman *et al.*, 2014). Meteoric water is also unlikely to penetrate the brittle/ductile transition in sufficient volumes to alter the  $\delta^{18}\text{O}$  value of the country rocks (e.g. Menzies *et al.*, 2014). This transition is at a depth of 5–10 km in the Basin and Range province today (Gans, 1987), and we consider this, or perhaps even shallower depths (due to very high heat flow), to likely reflect conditions in CRB times as well. We prefer this to the model of Leeman *et al.* (2008), which proposes a deeper ‘sweet spot’ for low- $\delta^{18}\text{O}$  magma generation at 15 km depth.

The low- $\delta^{18}\text{O}$  syn-CRB rhyolites erupted in regions that were experiencing syn-volcanic extension, particularly along a north–south trending series of grabens that includes the

Oregon–Idaho graben and the Northern Nevada Rift (Fig. 1, Ferns and McClaughry, 2013). This east–west extension is also recorded by the orientation of the majority of CRB dikes. The oldest low- $\delta^{18}\text{O}$  syn-CRB rhyolite dated so far – the 15.9 Ma (Benson *et al.*, 2013) Tuff of Leslie Gulch ( $\delta^{18}\text{O}_{\text{melt}} = +4.8\text{‰}$ , and with zircon as low as  $+1.95\text{‰}$ ) – erupted coevally with the early stages of normal faulting in the Oregon–Idaho graben. More  $\delta^{18}\text{O}$ -depleted rhyolites, such as the Rhyolite of Cottonwood Mountain ( $\delta^{18}\text{O}_{\text{melt}} = +1.9\text{‰}$  in one sample), erupted along the western graben-bounding faults after more subsidence had taken place (Cummings *et al.*, 2000). Another low- $\delta^{18}\text{O}$  area, the J-P Desert, discussed in detail in Colón *et al.* (2015), also erupted coevally with Basin and Range extension, which started in the region at ~16 Ma (Brueseke *et al.*, 2014; Colón *et al.*, 2015; and references therein). These extensional faults provided conduits for meteoric water to penetrate the crust and produce low- $\delta^{18}\text{O}$  rocks that were then melted to form syn-

CRB rhyolites (Figure 4, Gottardi *et al.*, 2013), and there is evidence for the presence of lakes in the Oregon–Idaho graben while these faults were active (Cummings *et al.*, 2000). The heat needed to drive the exchange of oxygen isotopes between the rock and the invading meteoric water would have been provided by the intrusion of the CRB magmas, the waning stages of which erupted coeval with the Oregon–Idaho graben rhyolites (Cummings *et al.*, 2000; Coble and Mahood, 2012; Ferns and McClaughry, 2013). This normal faulting-based mechanism for low- $\delta^{18}\text{O}$  rhyolite formation was also proposed in studies made individually for the Lake Owyhee, Santa Rosa-Calico and J-P Desert syn-CRB rhyolite centres, and the Picabo centre in the Snake River Plain (Amrhein *et al.*, 2013; Blum *et al.*, 2013; Drew *et al.*, 2013; Colón *et al.*, 2015). The lack of voluminous low- $\delta^{18}\text{O}$  rhyolites at the Northern Nevada Rift, despite syn-volcanic normal faulting there, may have been a result of less available heat for hydrothermal alteration there compared with the Oregon–Idaho graben, which was closer to the putative

axis of the mantle plume. Instead, relatively unaltered crust melted to produce the predominantly high- $\delta^{18}\text{O}$  rhyolites of the Northern Nevada Rift.

By compiling deviations from mantle values towards different crustal end-members, our isotopic study of the syn-CRB rhyolites ‘maps’ pre-existing crust types, and particularly maps those areas that experienced syn-volcanic hydrothermal alteration. The Oregon–Idaho graben, which is the site of the most voluminous low- $\delta^{18}\text{O}$  rhyolite volcanism, is on the edge of the suture zone between accreted Palaeozoic terranes and the ancient North American craton (Leeman *et al.*, 1992; Dorsey and LaMaskin, 2008; Shervais and Hanan, 2008). Similarly, the other sites of low- $\delta^{18}\text{O}$  volcanism are located in or near this transition zone, which is marked on the surface by the  $^{87}\text{Sr}/^{86}\text{Sr} = 0.706$  and 704 isopleths (Fig. 1), and reflected by diverse Hf isotopes in zircons in rhyolites from this transition zone (Fig. 3).

These isotopic observations corroborate numerical models of plume interactions with continental lithosphere. In particular, Burov *et al.* (2007) showed that lithospheric warping and gradients in surface uplift above a mantle plume will be concentrated by a lithospheric thickness transition, as the plume stalls against the thicker lithosphere and causes greater uplift in the thin lithosphere (Fig. 3). This concentration of deformation, which can produce conduits for magma and hydrothermal fluids via shallow faulting, is illustrated by the eruption of a majority of the syn-CRB rhyolites, including the great majority of low- $\delta^{18}\text{O}$  rhyolites, through the crustal transition zone that represents the transition between thin accreted terranes and the North American craton (Figs 1 and 3). In addition, it appears that broader regional extension in the northwest Basin and Range province, which began nearly simultaneously with the eruption of the CRB (Colgan and Henry, 2009), was triggered by the heat from the mantle plume underplating and thermally weakening the overthickened and pre-stressed continental lithosphere (e.g. Burov and Geyra, 2014; Camp *et al.*, 2015). Hence, the Yellowstone

mantle plume produced the normal faulting in the suture region, the heat to drive hydrothermal alteration in those faults, and the further heat to melt the crust and produce both high- and low- $\delta^{18}\text{O}$  rhyolites in compositionally diverse crust. This interplay between a mantle plume, extensional tectonics and the production of low- $\delta^{18}\text{O}$  rhyolites with diverse zircons has been observed today in Iceland (e.g. Bindeman *et al.*, 2012). This suggests that mantle plumes may have played a significant role, via hydrothermal preconditioning and melting, in the evolution of continental crust throughout geological history.

### Acknowledgements

We thank Mark Ferns and Chris Henry for invaluable help via their mapping efforts and personal assistance with locating outcrops, Jade Star Lackey and Scott Boroughs for trace element analyses, and Martin Streck and Matthew Loewen for helpful discussions, and reviews by R.J. Pankhurst and an additional anonymous reviewer. This study was supported by NSF grant EAR/CAREER-844772.

### References

- Amrhein, K.E., Brueseke, M.E. and Larson, P.B., 2013. *Oxygen isotope constraints on mid-Miocene rhyolite production in the Santa Rosa-Calico volcanic field, NV*. Abstract, Geological Society of America Annual Meeting.
- Benson, T.R., Mahood, G.A. and Grove, M., 2013. New geologic and geochronologic data on the Lake Owyhee Volcanic Field, Oregon: A silicic center contemporaneous with flood basalt volcanism. Abstract, Geological Society of America Cordilleran Section 2013 Annual Meeting.
- Bindeman, I.N., 2008. Oxygen Isotopes in Mantle and Crustal Magmas as Revealed by Single Crystal Analysis. *Rev. Mineral. Geochem.*, **69**, 445–478.
- Bindeman, I. and Simakin, A., 2014. Rhyolites – hard to produce but easy to recycle and sequester: bringing together microgeochemical observations and numerical methods. *Geosphere*, **10**, 930–957.
- Bindeman, I., Gurenko, A., Carley, T., Miller, C., Martin, E. and Sigmarrsson, O., 2012. Silicic magma petrogenesis in Iceland by remelting of hydrothermally altered crust based on oxygen isotope diversity and disequilibria between zircon and magma with implications for MORB. *Terra Nova*, **24**, 227–232.
- Blum, T., Kitajima, K., Nakashima, D. and Valley, J.W., 2013. Oxygen isotope evolution of the Lake Owyhee volcanic field, Oregon, and implications for low- $\delta^{18}\text{O}$  magmas of the Snake River Plain-Yellowstone hotspot. Abstract, American Geophysical Union Fall Meeting 2013.
- Brueseke, M.E., Callicot, J.S., Hames, W. and Larson, P.B., 2014. Mid-Miocene volcanism in northeastern Nevada: the Jarbidge Rhyolite and its relationship to Cenozoic evolution of the northern Great Basin (USA). *Geol. Soc. Am. Bull.*, **126**, 1047–1067.
- Bryan, S.E. and Ferrari, L., 2013. Large igneous provinces and silicic large igneous provinces: progress in our understanding over the last 25 years. *Geol. Soc. Am. Bull.*, **127**, 1053–1078.
- Burov, E. and Geyra, T., 2014. Asymmetric three-dimensional topography over mantle plumes. *Nature*, **513**, 85–89.
- Burov, E., Guillow-Frotier, L., d'Acremont, E., Le Pourheit, L. and Cloetingh, S., 2007. Plume head-lithosphere interactions near intra-continental plate boundaries. *Tectonophysics*, **434**, 15–38.
- Camp, V.E. and Hanan, B.B., 2008. A plume-triggered delamination origin for the Columbia River Basalt Group. *Geosphere*, **4**, 480–495.
- Camp, V.E. and Ross, M.E., 2004. Mantle dynamics and genesis of mafic magnetism in the intermontane Pacific Northwest. *J. Geophys. Res.*, **109**, B08204.
- Camp, V.E., Ross, M.E. and Hanson, W.E., 2003. Genesis of flood basalts and Basin and Range volcanic rocks from Steens Mountain to the Malheur River Gorge, Oregon. *Geol. Soc. Am. Bull.*, **115**, 105–128.
- Camp, V.E., Pierce, K.L. and Morgan, L.A., 2015. Yellowstone plume trigger for Basin and Range extension, and coeval emplacement of the Nevada-Columbia Basin magmatic belt. *Geosphere*, **???**, ???–???
- Carlson, R.W., 1984. Isotopic constraints on Columbia River flood basalt genesis and the nature of the subcontinental mantle. *Geochim. Cosmochim. Acta*, **48**, 2357–2372.
- Coble, M.A. and Mahood, G.A., 2012. Initial impingement of the Yellowstone plume located by widespread silicic volcanism contemporaneous with Columbia River flood basalts. *Geology*, **40**, 655–658.
- Colgan, J.P. and Henry, C.D., 2009. Rapid middle Miocene collapse of the Mesozoic orogenic plateau in north-central Nevada. *Int. Geol. Rev.*, **51**, 920–961.
- Colón, D.P., Bindeman, I.N., Ellis, B.S., Schmitt, A.K. and Fisher, C.M., 2015. Hydrothermal alteration and melting of the crust during the Columbia River Basalt-Snake River Plain transition and the origin of low- $\delta^{18}\text{O}$  rhyolites of the central Snake River Plain. *Lithos*, **224–225**, 310–323.
- Cummings, M.L., Evans, J.G., Ferns, M.L. and Lees, K.R., 2000. Stratigraphic and structural evolution of the middle-Miocene synvolcanic Oregon-Idaho graben. *Geol. Soc. Am. Bull.*, **112**, 63–77.
- Dorsey, R.J. and LaMaskin, T.A., 2008. Mesozoic collision and accretion of accreted terranes in the Blue Mountains province of northeastern Oregon. New insights from the stratigraphic record. *Arizona Geol. Soc. Dig.*, **22**, 325–332.
- Drew, D.L., Bindeman, I.N., Watts, K.E., Schmitt, A.K., Fu, B. and McCurry, M., 2013. Crustal-scale recycling in calderas and rift zones along the Yellowstone hotspot track: O and Hf isotopic evidence in diverse zircons from voluminous rhyolites of the Picabo volcanic field, Idaho. *Earth Planet. Sci. Lett.*, **381**, 63–77.
- Duncan, R.A., 1982. A captured island chain in the Coast Range of Oregon and Washington. *J. Geophys. Res. Solid Earth*, **87**(B13), 10827–10837.
- Ellis, B.S., Wolff, J.A., Boroughs, S., Mark, D.F., Starkel, W.A. and Bonnicksen, B., 2013. Rhyolitic volcanism of the central Snake River Plain: a review. *Bull. Volcanol.*, **75**, 1–19.
- Ferns, M.L. and McClaughry, J.D., 2013. Stratigraphy and volcanic evolution of the middle Miocene to Pliocene La Grande-Owyhee eruptive axis in eastern Oregon. In: *The Columbia River Flood Basalt Province* (S.P. Reidel, V.E. Camp, M.E. Ross, J.A. Wolff, B.S. Martin, T.L. Tolan and R.E. Wells, eds). *Geol. Soc. Am. Spec. Pap.*, **497**, 401–427.
- Gans, P.B., 1987. An open-system, two-layer crustal stretching model for the eastern Great Basin. *Tectonics*, **6**, 1–12.
- Glen, J.M.G. and Ponce, D.A., 2002. Large-scale fractures related to the inception of the Yellowstone hotspot. *Geology*, **30**, 647–650.
- Gottardi, R., Kao, P., Saar, M.O. and Tessier, C., 2013. Effects of permeability fields on fluid, heat, and oxygen isotope transport in extensional detachment systems. *Geochem. Geophys. Geosyst.*, **14**, 1493–1522.
- Hooper, P.R. and Hawkesworth, C.J., 1993. Isotopic and Geochemical Constraints on the Origin and Evolution of the Columbia River Basalt. *J. Petrol.*, **34**, 1203–1246.
- Jenkins, E.N., Streck, M.J., Ramos, F.C. and Bindeman, I.N., 2013. Radiogenic and stable isotopes of mid-Miocene

- silicic volcanism in eastern Oregon: Evidence for variable and high Sr/low d18O domains west of the terrane-cratonic lithosphere transition. Abstract. Geological Society of America Fall Meeting 2013.
- Leeman, W.P., 1982. Evolved and hybrid lavas from the Snake River Plain, Idaho. In: *Cenozoic Geology of Idaho* (B. Bonnicksen and R.B. Breckenridge, eds). *Idaho Bureau Mines Geol. Bull.*, **26**, 193–202.
- Leeman, W.P., Oldow, J.S. and Hart, W.K., 1992. Lithosphere-scale thrusting in the western U.S. Cordillera as constrained by Sr and Nd isotopic transitions in Neogene volcanic rocks. *Geology*, **23**, 63–66.
- Leeman, W.P., Annen, C. and Dufek, J., 2008. Snake River Plain–Yellowstone silicic volcanism: implications for magma generation and magma fluxes. In: *Dynamics of Crustal Magma Transfer, Storage, and Differentiation* (C. Annen and G.F. Zellmer, eds). *Geol. Soc. London Spec. Publ.*, **304**, 235–259.
- Mallis, J.D., Mahood, G.A. and Valley, J.W., 2014.  $\delta^{18}\text{O}$  of rhyolites at High Rock caldera complex, NW Nevada: Implications for silicic magma genesis associated with mid-Miocene flood basalts. Geological Society of America Rocky Mountain and Cordilleran Joint Meeting 2014.
- McCurry, M. and Rodgers, D.W., 2009. Mass transfer along the Yellowstone hotspot track I: petrologic constraints on the volume of mantle-derived magma. *J. Volcanol. Geoth. Res.*, **188**, 86–98.
- Menzies, C.D., Teagle, D.A.H., Craw, D., Cox, S.C., Boyce, A.J., Barrie, C.D. and Roberts, S., 2014. Incursion of meteoric waters into the ductile regime in an active orogeny. *Earth Planet. Sci. Lett.*, **399**, 1–13.
- Nash, B.P., Perkins, M.E., Christensen, J.N., Lee, D. and Halliday, A.N., 2006. The Yellowstone hotspot in space and time: Nd and Hf isotopes in silicic magmas. *Earth Planet. Sci. Lett.*, **247**, 143–156.
- Norton, D. and Taylor, H.P., 1979. Quantitative simulation of the hydrothermal systems of crystallizing magmas on the basis of transport theory and oxygen isotope data: an analysis of the Skaergaard intrusion. *J. Petrol.*, **20**, 421–486.
- Reidel, S.P., Camp, V.E., Tolan, T.L. and Martin, B.S., 2013. The Columbia River flood basalt province: stratigraphy, areal extent, volume, and physical volcanology. In: *The Columbia River Flood Basalt Province* (S.P. Reidel, V.E. Camp, M.E. Ross, J.A. Wolff, B.S. Martin, T.L. Tolan and R.E. Wells, eds). *Geol. Soc. Am. Spec. Pap.*, **497**, 1–43.
- Schmandt, B., Dueker, K., Humphreys, E. and Hansen, S., 2012. Hot mantle upwelling across the 660 beneath Yellowstone. *Earth Planet. Sci. Lett.*, **331**, 224–236.
- Seligman, A.N., Bindeman, I.N., McLaughry, J., Stern, R.A. and Fisher, C., 2014. The earliest low and high  $\delta^{18}\text{O}$  caldera-forming eruptions of the Yellowstone plume: implications for the 30–40 Ma Oregon calderas and speculations on plume-triggered delaminations. *Front. Earth Sci.*, **2**, ???–???.
- Shervais, J.W. and Hanan, B.B., 2008. Lithospheric topography, tilted plumes, and the track of the Snake River–Yellowstone hot spot. *Tectonics*, **27**, TC5004.
- Taylor, H.P., 1974. The application of oxygen and hydrogen isotope studies to problems of hydrothermal alteration and ore deposition. *Econ. Geol.*, **69**, 843–883.
- Wolff, J.A. and Ramos, F.C., 2013. Source materials for the main phase of the Columbia River Basalt Group: geochemical evidence and implication for magma storage and transport. In: *The Columbia River Flood Basalt Province* (S.P. Reidel, V.E. Camp, M.E. Ross, J.A. Wolff, B.S. Martin, T.L. Tolan and R.E. Wells, eds). *Geol. Soc. Am. Spec. Pap.*, **497**, 273–292.
- Wolff, J.A., Ramos, F.C., Hart, G.L., Patterson, J.D. and Brandon, A.D., 2008. Columbia River flood basalts from a centralized crustal magmatic system. *Nat. Geosci.*, **1**, 177–180.

Received 8 December 2014; revised version accepted 29 April 2015

### Supporting Information

Additional Supporting Information may be found in the online version of this article:

- Data S1.** Detailed methods.
- Data S2.** Sources of data for Figure 1.
- Data S3.** Sources of data for Figures 2 and 3 and Table S2.
- Data S4.** Sample descriptions.
- Data S5.** Figures and Tables.
- Data S6.** References for Supplementary Material.